

# Adjoint Estimation of the Variation in a Model Functional

## Output Due to Assimilation of Data

DACIAN N. DAESCU \*

*Portland State University, Portland, Oregon*

RICARDO TODLING<sup>†</sup>

*Global Modeling and Assimilation Office, NASA/GSFC, Greenbelt, Maryland*

---

\* *Corresponding author address:* Dr. Dacian N. Daescu, Department of Mathematics and Statistics,  
Portland State University, P.O. Box 751, Portland, OR 97207, U.S.A.

E-mail: daescu@pdx.edu

<sup>†</sup> *Additional Affiliation:* Sciences Applications International Corporation, Bestville, Maryland.

## ABSTRACT

A parametric approach to the adjoint estimation of the variation in a model functional output due to assimilation of data is considered as a tool to analyze and develop observation impact measures. The parametric approach is specialized to a linear analysis scheme and it is used to derive various high-order approximation equations. This framework includes Kalman filter and incremental three- and four-dimensional variational data assimilation schemes implementing a single outer loop iteration. Distinction is made between Taylor series methods and numerical quadrature methods. The novel quadrature approximations require minimal additional software development and are suitable for testing and implementation at operational numerical weather prediction centers where a data assimilation system (DAS) and the associated adjoint DAS are in place. Their potential use as tools for observation impact estimates needs to be further investigated. Preliminary numerical experiments are provided using NASA Goddard Earth Observing System (GEOS-5) atmospheric DAS.

# 1. Introduction

An optimal use of the increasing amounts of atmospheric data in numerical weather prediction (NWP) applications and the design of future observing networks require the development of efficient data analysis tools to quantify the "value" added by observations to a specific data assimilation system (DAS) and model forecast. A judicious assessment of the observation value must account for the data location in the time-space domain, observation type, instrument type, as well as data interaction in the presence of multiple observing systems. Estimation of the observation impact on the short-range model forecast may be performed through observing system experiments (OSE's, Atlas 1997) where selected data sets are systematically added or removed from the assimilation procedure (Kelly et al. 2007). This approach is suitable when the impact of a few data subsets is investigated and becomes computationally prohibitive when the impact of a large number of data subsets or of all individual measurements is considered.

Adjoint-based observation sensitivity, initially developed in NWP as an observation-targeting tool (Baker and Daley 2000, Doerenbecher and Bergot 2001), provides a feasible (all-at-once) approach to the observation impact estimation for a large variety of data sets and individual observations. Techniques based on observation sensitivity are currently used to monitor the impact of observations provided by the routine observing systems on a selected short-range forecast aspect and to assess the efficiency of various observation-targeting strategies (Fourrié et al. 2002, Langland and Baker 2004, Langland 2005, Gelaro et al. 2007, Zhu and Gelaro 2008). Estimation of observation impact in an ensemble Kalman filter data assimilation scheme is discussed by Liu and Kalnay (2008).

The observation impact estimation relies on the chain rule relationship: the change in a scalar forecast measure  $e$  (e.g., forecast error) is due to the changes in the initial conditions as a result of the data assimilation procedure. The analysed forecast is implicitly a function of observations and adjoint modeling is used to provide an explicit estimate of the variation  $\delta e$  in terms of the innovation vector in the observation space.

The necessity of considering higher-than-first-order approximations is discussed by Errico (2007, hereafter E07) and Gelaro et al. (2007, hereafter GZE07) who derive various-order approximation schemes and analyze the results using the NASA Goddard Earth Observing System forecast model and DAS. The approach developed by Langland and Baker (2004, hereafter LB04) and first implemented in the Naval Research Laboratory DAS provides an observation impact estimate based on a higher order approximation to the variation  $\delta e$  in the forecast error (with error of third order, as shown in E07) by combining adjoint sensitivity gradients from two trajectories: background and analysis. The potential of the nonlinear approximations to introduce ambiguities in the impact estimates of individual observations is investigated in E07 and GZE07. In their studies it is also emphasized that further research in the design of new observation impact measures is required and that a judicious theoretical framework to high-order observation impact estimation is yet to be formulated.

In the present work a parametric approach to the adjoint estimation of the variation in a model functional output due to assimilation of data is considered as a tool to analyze and develop observation impact measures. The parametric approach is specialized to a linear analysis scheme and it is used to derive various  $\delta e$ -approximation equations. This framework includes Kalman filter and incremental three- and four-dimensional variational data assimilation schemes (3D-Var, 4D-Var) implementing a single outer loop iteration (Daley 1991,

Courtier et al. 1994). Distinction is made between Taylor series methods and numerical quadrature methods. The novel quadrature approximations derived in this study require a minimal additional software development and are suitable for testing and implementation at operational NWP centers where data assimilation schemes and the associated adjoint DAS are in place. Their potential use as tools for observation impact estimates needs to be further investigated.

Section 2 includes a brief review of current adjoint-based observation impact measures in data assimilation. The parametric methodology to adjoint estimation of the variation in model functional output due to assimilation of data is described in section 3; a table of approximation formulae is provided together with an order analysis and the associated error estimates. Preliminary numerical results are presented in section 4 using the fifth generation NASA Goddard Earth Observing System (GEOS-5) atmospheric DAS. Summary and further research directions are in section 5.

## 2. Adjoint-based observation impact measures

Consider a data assimilation scheme that provides an optimal estimate (analysis)  $\mathbf{x}_a$  to the initial conditions of an atmospheric model (Daley 1991, Kalnay 2002)

$$\mathbf{x}_a = \mathbf{x}_b + \mathbf{K}[\mathbf{y} - \mathbf{h}(\mathbf{x}_b)] \quad (1)$$

where  $\mathbf{x}_b$  is a background estimate to the initial conditions,  $\mathbf{y}$  is the vector of observational data,  $\mathbf{h}$  is the observation operator and

$$\mathbf{K} = \mathbf{B}\mathbf{H}^T [\mathbf{H}\mathbf{B}\mathbf{H}^T + \mathbf{R}]^{-1} \quad (2)$$

is the optimal gain matrix expressed in terms of the background error covariance matrix  $\mathbf{B}$ , the observation error covariance matrix  $\mathbf{R}$ , and the linearized observation operator  $\mathbf{H}$ . Denoting the analysis increment  $\delta\mathbf{x}_a = \mathbf{x}_a - \mathbf{x}_b$  and the innovation vector  $\delta\mathbf{y} = \mathbf{y} - \mathbf{h}(\mathbf{x}_b)$ , the analysis equation (1) is written

$$\delta\mathbf{x}_a = \mathbf{K}\delta\mathbf{y} \quad (3)$$

The analysis provided by Kalman filter-based methods as well as incremental 3D-Var and 4D-Var schemes implementing a single outer loop iteration is formally expressed as (3).

The observation sensitivity and impact estimation are specific to a forecast aspect of interest. A typical scalar measure of the error in a forecast initiated from  $\mathbf{x}_0$  is defined (LB04, GZE07)

$$e(\mathbf{x}_0) = (\mathbf{x}_0^f - \mathbf{x}^t)^T \mathbf{C}(\mathbf{x}_0^f - \mathbf{x}^t) \quad (4)$$

where  $\mathbf{x}_0^f = \mathcal{M}(\mathbf{x}_0)$  is the nonlinear model forecast at time  $t$  initiated at  $t_0 < t$  from  $\mathbf{x}_0$ ,  $\mathbf{x}^t$  is the verifying analysis at time  $t$ , the superscript  $T$  denotes the transpose operator, and  $\mathbf{C}$  is a symmetric and positive definite matrix that defines the metric on the state space e.g., an appropriate energy norm.

For the purpose of this work we consider a general model functional output  $e(\mathbf{x}_0)$ , assumed to be a smooth function of the initial conditions. The change in  $e$  due to assimilation of data is

$$\delta e = e(\mathbf{x}_a) - e(\mathbf{x}_b) \quad (5)$$

In particular, for the forecast error measure (4)

$$\delta e = (\mathbf{x}_a^f - \mathbf{x}^t)^T \mathbf{C}(\mathbf{x}_a^f - \mathbf{x}^t) - (\mathbf{x}_b^f - \mathbf{x}^t)^T \mathbf{C}(\mathbf{x}_b^f - \mathbf{x}^t) \quad (6)$$

and the gradient of  $e$  evaluated at  $\mathbf{x}_0 = \mathbf{x}_a$  and  $\mathbf{x}_0 = \mathbf{x}_b$  is expressed, respectively

$$\nabla_{\mathbf{x}_0} e(\mathbf{x}_a) = 2\mathbf{M}^T(\mathbf{x}_a)\mathbf{C}(\mathbf{x}_a^f - \mathbf{x}^t), \quad (7)$$

$$\nabla_{\mathbf{x}_0} e(\mathbf{x}_b) = 2\mathbf{M}^T(\mathbf{x}_b)\mathbf{C}(\mathbf{x}_b^f - \mathbf{x}^t) \quad (8)$$

In eqs. (7) and (8),  $\mathbf{M}^T(\mathbf{x}_a)$  and  $\mathbf{M}^T(\mathbf{x}_b)$  denote the adjoint of the tangent linear model from  $t_0$  to  $t$  evaluated along the analysis trajectory and background trajectory, respectively.

To a first order approximation, from eqs. (3) and (5) the variation  $\delta e$  due to assimilation of data  $\mathbf{y}$  may be estimated using a linearization around the background  $\mathbf{x}_b$

$$\delta e \approx (\delta\mathbf{x}_a)^T \nabla_{\mathbf{x}_0} e(\mathbf{x}_b) = (\delta\mathbf{y})^T \mathbf{K}^T \nabla_{\mathbf{x}_0} e(\mathbf{x}_b) \stackrel{def}{=} \delta e_1^b \quad (9)$$

or, alternatively, using a linearization around the analysis  $\mathbf{x}_a$

$$\delta e \approx (\delta\mathbf{x}_a)^T \nabla_{\mathbf{x}_0} e(\mathbf{x}_a) = (\delta\mathbf{y})^T \mathbf{K}^T \nabla_{\mathbf{x}_0} e(\mathbf{x}_a) \stackrel{def}{=} \delta e_1^a \quad (10)$$

The measure (10) has been initially considered for observation impact studies since it relates directly to the concept of observation sensitivity introduced in Baker and Daley (2000).

From (1) the analysis sensitivity to observations is expressed

$$\nabla_{\mathbf{y}} \mathbf{x}_a = \mathbf{K}^T \quad (11)$$

Chain rule differentiation provides the sensitivity of the forecast initiated from  $\mathbf{x}_a$  to observations

$$\nabla_{\mathbf{y}} e(\mathbf{x}_a) = \nabla_{\mathbf{y}} \mathbf{x}_a \nabla_{\mathbf{x}_0} e(\mathbf{x}_a) = \mathbf{K}^T \nabla_{\mathbf{x}_0} e(\mathbf{x}_a) \quad (12)$$

and from (10) and (12) it follows

$$\delta e_1^a = (\delta\mathbf{y})^T \nabla_{\mathbf{y}} e(\mathbf{x}_a) \quad (13)$$

such that  $\delta e_1^a$  is the inner product in the observation space between the innovation vector and the observation sensitivity vector. The observation impact methodology first introduced in LB04 estimates the variation  $\delta e$  using sensitivity gradients along both background and analysis trajectories

$$\delta e \approx (\delta \mathbf{y})^T \mathbf{K}^T \left[ \frac{1}{2} \nabla_{\mathbf{x}_0} e(\mathbf{x}_a) + \frac{1}{2} \nabla_{\mathbf{x}_0} e(\mathbf{x}_b) \right] \stackrel{def}{=} \delta e_2^{a,b} \quad (14)$$

which is a *second order accurate* (error of third order) approximation to  $\delta e$ , as shown in E07 and in section 3a below.

**Remark 1.** In the  $\delta e$ -approximation measures derived throughout this work a subscript is used to specify *the order of accuracy* and a superscript is used to specify the trajectories involved in the computation. In LB04  $\delta e_2^{a,b}$  is denoted  $\delta e_f^g$ , whereas E07 and GZE07 use the notation  $\delta e_3$  to specify the same expression.

**Remark 2.** From eqs. (9), (10), and (14) one notices that  $\delta e_2^{a,b}$  may be obtained by averaging the first order approximations  $\delta e_1^a$  and  $\delta e_1^b$ . This property is also reflected in the tables of numerical data provided in GZE07.

With an appropriate definition of the response functional  $e$ , the measures  $\delta e_1^a$  and  $\delta e_2^{a,b}$  have been used by Fourrié et al. (2002), Zhu and Gelaro (2008), Langland and Baker (2004), Langland (2005) to assess the impact of individual data components in the assimilation scheme by taking the element-wise product between the innovation vector and the corresponding  $\delta \mathbf{y}$ -amplification factor. The validity and the appropriate use of these approximations as well as the interpretation of the "observation impact" are thus closely determined by the forecast model  $\mathcal{M}$  and the specification of the model functional output  $e$ . Various-order observation impact measures are analysed in GZE07, including  $\delta e_1^b$  and  $(1/2)\delta e_1^b$ . A

relationship between the measures  $\delta e_2^{a,b}$  and  $(1/2)\delta e_1^b$  is further discussed in appendix.

The experience gained from the above-mentioned studies is that in practice first-order estimates are not accurate approximations to the variation  $\delta e$  in the forecast aspect due to assimilation of data. In the next section a parametric approach is considered to obtain high-order  $\delta e$ -approximations and it is used to derive various adjoint-based approximation schemes, determine their order of accuracy, and provide the associated error estimates.

### 3. High-order adjoint-based estimation to $\delta e$

Consider a family of suboptimal analyses defined by a parameter  $s, 0 \leq s \leq 1$ :

$$\mathbf{x}(s) \stackrel{def}{=} \mathbf{x}_b + s(\mathbf{x}_a - \mathbf{x}_b) = \mathbf{x}_b + s\mathbf{K}\delta\mathbf{y} \quad (15)$$

such that  $\mathbf{x}(0) = \mathbf{x}_b$  and  $\mathbf{x}(1) = \mathbf{x}_a$ . The midpoint of the segment from  $\mathbf{x}_b$  to  $\mathbf{x}_a$  is denoted

$$\mathbf{x}(1/2) = \frac{1}{2}(\mathbf{x}_b + \mathbf{x}_a) \stackrel{def}{=} \mathbf{x}_{(a+b)/2} \quad (16)$$

Corresponding to (15) and to the model functional output  $e$  we associate the function

$$\hat{e} : [0, 1] \rightarrow \mathbb{R}, \quad \hat{e}(s) \stackrel{def}{=} e(\mathbf{x}(s)) \quad (17)$$

As the parameter  $s$  describes the segment  $[0, 1]$  on the real axis,  $\mathbf{x}(s)$  describes the segment from  $\mathbf{x}_b$  to  $\mathbf{x}_a$  in the state space; accordingly, the function  $\hat{e}$  evolves from  $\hat{e}(0)$  to  $\hat{e}(1)$  and the model functional output evolves from  $e(\mathbf{x}_b)$  to  $e(\mathbf{x}_a)$  such that the variation  $\delta\hat{e}$  is identical to the variation  $\delta e$ :

$$\delta\hat{e} = \hat{e}(1) - \hat{e}(0) = e(\mathbf{x}_a) - e(\mathbf{x}_b) = \delta e \quad (18)$$

The process is illustrated in Fig. 1. Taking into account that  $\mathbf{x}(s)$  depends linearly on  $s$  and has a constant derivative

$$\mathbf{x}'(s) = \mathbf{K}\delta\mathbf{y}, \quad 0 \leq s \leq 1, \quad (19)$$

from (17) and (19) using chain rule differentiation the first and second order derivatives of  $\hat{e}$  are expressed respectively,

$$\hat{e}'(s) = (\delta\mathbf{y})^T \mathbf{K}^T \nabla_{\mathbf{x}_0} e(\mathbf{x}(s)), \quad 0 \leq s \leq 1 \quad (20)$$

$$\hat{e}''(s) = (\delta\mathbf{y})^T \mathbf{K}^T \nabla_{\mathbf{x}_0}^2 e(\mathbf{x}(s)) \mathbf{K} \delta\mathbf{y}, \quad 0 \leq s \leq 1 \quad (21)$$

where  $\nabla_{\mathbf{x}_0}^2 e(\mathbf{x}(s))$  denotes the Hessian matrix of  $e$  with respect to initial conditions, evaluated at  $\mathbf{x}(s)$ . In particular,

$$\hat{e}'(0) = (\delta\mathbf{y})^T \mathbf{K}^T \nabla_{\mathbf{x}_0} e(\mathbf{x}_b), \quad \hat{e}''(0) = (\delta\mathbf{y})^T \mathbf{K}^T \nabla_{\mathbf{x}_0}^2 e(\mathbf{x}_b) \mathbf{K} \delta\mathbf{y} \quad (22)$$

$$\hat{e}'(1) = (\delta\mathbf{y})^T \mathbf{K}^T \nabla_{\mathbf{x}_0} e(\mathbf{x}_a), \quad \hat{e}''(1) = (\delta\mathbf{y})^T \mathbf{K}^T \nabla_{\mathbf{x}_0}^2 e(\mathbf{x}_a) \mathbf{K} \delta\mathbf{y} \quad (23)$$

In general, the  $m$ -order derivatives of  $\hat{e}$  are expressed in terms of the gain matrix  $\mathbf{K}$ , the innovation vector  $\delta\mathbf{y}$ , and the  $m$ -order derivatives of the functional  $e$  with respect to initial conditions, evaluated at  $\mathbf{x}(s)$ :

$$\hat{e}^m(s) = \nabla_{\mathbf{x}_0}^m e(\mathbf{x}(s)) \cdot (\mathbf{K}\delta\mathbf{y})^m, \quad 0 \leq s \leq 1 \quad (24)$$

where the right side term in (24) is defined recursively

$$\nabla_{\mathbf{x}_0} e(\mathbf{x}(s)) \cdot (\mathbf{K}\delta\mathbf{y}) = (\delta\mathbf{y})^T \mathbf{K}^T \nabla_{\mathbf{x}_0} e(\mathbf{x}(s))$$

$$\nabla_{\mathbf{x}_0}^m e(\mathbf{x}(s)) \cdot (\mathbf{K}\delta\mathbf{y})^m = (\delta\mathbf{y})^T \mathbf{K}^T \nabla_{\mathbf{x}_0} [\nabla_{\mathbf{x}_0}^{m-1} e(\mathbf{x}(s)) \cdot (\mathbf{K}\delta\mathbf{y})^{m-1}], \quad m \geq 2$$

**Remark 3.** If the forecast model is linear,  $\mathcal{M} = \mathbf{M}$ , and a quadratic functional output (4) is considered then the Hessian  $\nabla_{\mathbf{x}_0}^2 e$  is a state independent matrix

$$\nabla_{\mathbf{x}_0}^2 e = 2\mathbf{M}^T \mathbf{C} \mathbf{M} \quad (25)$$

a. *The  $\delta e$ -approximation equations and their error estimates*

The fundamental theorem of calculus

$$\hat{e}(1) - \hat{e}(0) = \int_0^1 \hat{e}'(s) ds \quad (26)$$

together with the relationship (18) and eqs. (20-24) are used next to derive several high-order approximations to  $\delta e$  and to provide the associated error estimates based on Taylor series and the theory of numerical integration (Atkinson 1988). The error in the  $\delta e$ -approximation is expressed in terms of high-order derivatives of  $e$  with respect to the initial conditions evaluated at a certain point  $\mathbf{x}(\tau), 0 \leq \tau \leq 1$  in the state space, specific to each measure.

1) APPROXIMATIONS BASED ON TAYLOR SERIES AT  $\mathbf{x}_b$

i. First order accurate:  $\hat{e}(1) - \hat{e}(0) = \hat{e}'(0) + \frac{1}{2}\hat{e}''(\tau)$

$$\delta e_1^b = (\delta \mathbf{y})^T \mathbf{K}^T \nabla_{\mathbf{x}_0} e(\mathbf{x}_b) \quad (27)$$

$$\delta e - \delta e_1^b = \frac{1}{2}(\delta \mathbf{y})^T \mathbf{K}^T \nabla_{\mathbf{x}_0}^2 e(\mathbf{x}(\tau)) \mathbf{K} \delta \mathbf{y} \quad (28)$$

ii. Second order accurate:  $\hat{e}(1) - \hat{e}(0) = \hat{e}'(0) + \frac{1}{2}\hat{e}''(0) + \frac{1}{6}\hat{e}'''(\tau)$

$$\delta e_2^b = (\delta \mathbf{y})^T \mathbf{K}^T \nabla_{\mathbf{x}_0} e(\mathbf{x}_b) + \frac{1}{2}(\delta \mathbf{y})^T \mathbf{K}^T \nabla_{\mathbf{x}_0}^2 e(\mathbf{x}_b) \mathbf{K} \delta \mathbf{y} \quad (29)$$

$$\delta e - \delta e_2^b = \frac{1}{6} \nabla_{\mathbf{x}_0}^3 e(\mathbf{x}(\tau)) \cdot (\mathbf{K} \delta \mathbf{y})^3 \quad (30)$$

2) APPROXIMATIONS BASED ON TAYLOR SERIES AT  $\mathbf{x}_a$

i. First order accurate:  $\hat{e}(1) - \hat{e}(0) = \hat{e}'(1) - \frac{1}{2}\hat{e}''(\tau)$

$$\delta e_1^a = (\delta \mathbf{y})^T \mathbf{K}^T \nabla_{\mathbf{x}_0} e(\mathbf{x}_a) \quad (31)$$

$$\delta e - \delta e_1^a = -\frac{1}{2}(\delta \mathbf{y})^T \mathbf{K}^T \nabla_{\mathbf{x}_0}^2 e(\mathbf{x}(\tau)) \mathbf{K} \delta \mathbf{y} \quad (32)$$

ii. Second order accurate:  $\hat{e}(1) - \hat{e}(0) = \hat{e}'(1) - \frac{1}{2}\hat{e}''(1) + \frac{1}{6}\hat{e}'''(\tau)$

$$\delta e_2^a = (\delta \mathbf{y})^T \mathbf{K}^T \nabla_{\mathbf{x}_0} e(\mathbf{x}_a) - \frac{1}{2}(\delta \mathbf{y})^T \mathbf{K}^T \nabla_{\mathbf{x}_0}^2 e(\mathbf{x}_a) \mathbf{K} \delta \mathbf{y} \quad (33)$$

$$\delta e - \delta e_2^a = \frac{1}{6} \nabla_{\mathbf{x}_0}^3 e(\mathbf{x}(\tau)) \cdot (\mathbf{K} \delta \mathbf{y})^3 \quad (34)$$

3) APPROXIMATIONS BASED ON NUMERICAL QUADRATURE SCHEMES

Numerical quadrature schemes applied to (26) provide a  $\delta e$ -approximation

i. Second order accurate:

(a) Trapezoidal rule (LB04):

$$\begin{aligned} \int_0^1 \hat{e}'(s) ds &= \frac{1}{2}[\hat{e}'(0) + \hat{e}'(1)] - \frac{1}{12}\hat{e}'''(\tau) \\ \delta e_2^{a,b} &= \frac{1}{2}[\hat{e}'(0) + \hat{e}'(1)] = (\delta \mathbf{y})^T \mathbf{K}^T \frac{1}{2} [\nabla_{\mathbf{x}_0} e(\mathbf{x}_b) + \nabla_{\mathbf{x}_0} e(\mathbf{x}_a)] \end{aligned} \quad (35)$$

$$\delta e - e_2^{a,b} = -\frac{1}{12}\hat{e}'''(\tau) = -\frac{1}{12} \nabla_{\mathbf{x}_0}^3 e(\mathbf{x}(\tau)) \cdot (\mathbf{K} \delta \mathbf{y})^3 \quad (36)$$

(b) Midpoint rule:

$$\begin{aligned} \int_0^1 \hat{e}'(s) ds &= \hat{e}'(1/2) + \frac{1}{24}\hat{e}'''(\tau) \\ \delta e_2^{(a+b)/2} &= \hat{e}'(1/2) = (\delta \mathbf{y})^T \mathbf{K}^T \nabla_{\mathbf{x}_0} e(\mathbf{x}_{(a+b)/2}) \end{aligned} \quad (37)$$

$$\delta e - \delta e_2^{(a+b)/2} = \frac{1}{24}\hat{e}'''(\tau) = \frac{1}{24} \nabla_{\mathbf{x}_0}^3 e(\mathbf{x}(\tau)) \cdot (\mathbf{K} \delta \mathbf{y})^3 \quad (38)$$

ii. Fourth order accurate (Simpson's rule):

$$\begin{aligned} \int_0^1 \hat{e}'(s) ds &= \frac{1}{6}[\hat{e}'(0) + 4\hat{e}'(1/2) + \hat{e}'(1)] - \frac{1}{2880}\hat{e}^5(\tau) \\ \delta e_4^{a,b,(a+b)/2} &= \frac{1}{6}[\hat{e}'(0) + 4\hat{e}'(1/2) + \hat{e}'(1)] \\ &= (\delta \mathbf{y})^T \mathbf{K}^T \frac{1}{6} [\nabla_{\mathbf{x}_0} e(\mathbf{x}_b) + 4\nabla_{\mathbf{x}_0} e(\mathbf{x}_{(a+b)/2}) + \nabla_{\mathbf{x}_0} e(\mathbf{x}_a)] \end{aligned} \quad (39)$$

$$\delta e - \delta e_4^{a,b,(a+b)/2} = -\frac{1}{2880}\hat{e}^5(\tau) = -\frac{1}{2880}\nabla_{\mathbf{x}_0}^5 e(\mathbf{x}(\tau)) \cdot (\mathbf{K}\delta \mathbf{y})^5 \quad (40)$$

A summary of the adjoint-based approximations to the variation  $\delta e$  in the model functional output due to assimilation of data using a linear analysis scheme is in Table 1.

*b. Computational aspects and discussion*

Theoretically,  $\delta e$ -approximation formulae of any order may be derived using both Taylor series and numerical quadrature, however only the quadrature approach is (currently) feasible for the practical implementation of high-order estimates. Taylor series approximations to  $\delta e$  are expressed explicitly in terms of the innovation vector and derivatives at one of the endpoints  $\mathbf{x}_b$  or  $\mathbf{x}_a$ . The equations of the second order accurate approximations  $\delta e_2^b$  and  $\delta e_2^a$  clearly illustrate the presence of the innovation-component cross products  $(\delta y)_i(\delta y)_j$  in the higher-than-first order estimates. The quadrature schemes make use of information from both end nodes  $\mathbf{x}_b$  and  $\mathbf{x}_a$  such that implicitly the  $\delta \mathbf{y}$ -amplification factor associated to these schemes depends on all  $\delta \mathbf{y}$ 's components. Whether or not this trade-off may result in potential ambiguities when high-order  $\delta e$ -approximations are used to assess the impact of individual observation components needs to be further investigated (GZE07).

The Hessian-vector products involved in the second order Taylor series may be evaluated

with a second order adjoint model (Le Dimet et al. 2002) or approximated by gradient differences e.g.,  $\nabla_{\mathbf{x}_0}^2 e(\mathbf{x})\delta\mathbf{x}_a \approx [\nabla_{\mathbf{x}_0} e(\mathbf{x} + \epsilon\delta\mathbf{x}_a) - \nabla_{\mathbf{x}_0} e(\mathbf{x})]/\epsilon$ . Increasing the accuracy of quadrature approximations requires only additional adjoint model integrations along trajectories properly initiated on the segment from  $\mathbf{x}_b$  to  $\mathbf{x}_a$ . The midpoint equation (37) provides a second order accurate estimation to  $\delta e$  using *a single* gradient that is evaluated along the model trajectory initiated from  $\mathbf{x}_{(a+b)/2}$ . This point defined by (16) is obtained at virtually no additional computational cost once the analysis  $\mathbf{x}_a$  is available and, given the error estimates (36) and (38),  $\delta e_2^{(a+b)/2}$  may provide a potentially *more accurate approximation* to  $\delta e$  than the measure  $\delta e_2^{a,b}$ . Associated to the functional output (4) the measure  $\delta e_2^{(a+b)/2}$  is

$$\delta e_2^{(a+b)/2} = 2(\delta\mathbf{y})^T \mathbf{K}^T \mathbf{M}^T(\mathbf{x}_{(a+b)/2}) \mathbf{C}(\mathbf{x}_{(a+b)/2}^f - \mathbf{x}^t) \quad (41)$$

where  $\mathbf{x}_{(a+b)/2}^f$  is the forecast initiated from the midpoint  $\mathbf{x}_{(a+b)/2}$  and  $\mathbf{M}^T(\mathbf{x}_{(a+b)/2})$  is the adjoint model evaluated along the midpoint trajectory. In practice, when forecasts are issued for every analysis time, the state trajectories initiated from the background  $\mathbf{x}_b$  and the analysis  $\mathbf{x}_a$  can easily be made available, whereas obtaining the midpoint trajectory requires an additional run of the nonlinear forecast model. However, calculation of midpoint observation impact estimate requires only a single integration with the adjoint model  $\mathbf{M}^T$ , whereas the trapezoidal estimate requires two such integrations. The computational cost of implementing  $\delta e_2^{(a+b)/2}$  is thus roughly equivalent to the cost of implementing  $\delta e_2^{a,b}$ . The midpoint calculation may become more desirable in certain situations for instance, when using the impact calculation to tune an Observation System Simulation Experiment (OSSE; Errico personal comm.). In this case, forecasts are only issued with the sole purpose of calculating observation impact estimates, and therefore one might as well avoid the extra

adjoint model integration required to calculate the trapezoidal expression.

The Simpson's rule equation (39) gives a *fourth order accurate* (error of fifth order) estimate to  $\delta e$  at the expense of *only one additional forecast and adjoint model integration*, as compared to the second order accurate estimate  $\delta e_2^{a,b}$ . This measure provides a feasible tool for validating the observation sensitivity computations and for assessing the impact of the nonlinearities on the errors in the lower order approximations.

The error estimates provided in this section show that the accuracy of the  $\delta e$ -approximation measures depends on the innovation vector  $\delta \mathbf{y}$ , the DAS  $\mathbf{K}$ , the functional aspect  $e$ , the adjoint  $\mathbf{M}^T$ , and the high-order derivatives of the nonlinear forecast model. Theoretically, for linear dynamics and quadratic functional output all second-and-higher order accurate measures derived in this study provide the exact value of the variation  $\delta e$  and identical results when used for observation impact assessment.

To our knowledge, the measures (37) and (39) have not been previously considered for estimating the observation impact and whether or not these measures may provide viable tools for practical applications to observation impact studies needs to be further investigated. Their implementation requires no additional software development as compared e.g., to the observation impact estimates based on the  $\delta e_2^{a,b}$  measure and testing may be easily performed at operational NWP centers.

## 4. Illustrative numerical experiments

Preliminary numerical experiments are provided to illustrate the parametric approach to the analysis and design of observation impact measures using the fifth generation God-

standard Earth Observing System Data Assimilation System (GEOS-5; Rienecker et al. 2008). GEOS-5 assimilates observations using the incremental analysis update technique of Bloom et al. (1996). It consists of a global atmospheric model developed at Goddard and an analysis system developed jointly by the NOAA National Centers for Environmental Prediction (NCEP) and the NASA Global Modeling and Assimilation Office (GMAO). The atmospheric general circulation model (GCM) of GEOS-5 retains an updated version of the finite-volume hydrostatic dynamical core (Lin 2004) from its predecessor GEOS-4. The GEOS-5 GCM is built under the infrastructure of the Earth System Modeling Framework (Collins et al. 2005) used to couple together various physics packages including a modified version of the Relaxed Arakawa-Schubert convective parameterization scheme of Moorthi and Suarez (1992), the catchment-based hydrological model of Koster et al. (2000), the multi-layer snow model of Stieglitz et al. (2001), and the radiative transfer model of Chou and Suarez (1999). Furthermore, the GCM is accompanied by its adjoint model (ADM), which is essentially the ADM of the finite-volume dynamical core GEOS-4 (Giering et al., 2003), with added vertical diffusion and polar filter (Errico et al. 2007).

The GEOS-5 analysis component consists of the Gridpoint Statistical Interpolation (GSI) system. The GSI implements a 3D-Var using the incremental approach of Courtier et al. (1994) for minimization with the preconditioning strategy of Derber and Rosati (1989). The background error covariance is implemented as a series of recursive filters producing nearly Gaussian and isotropic correlation functions (Wu et al 2002). Satellite radiances are processed using the Community Radiative Transfer Model (CRTM; Kleespies et al. 2004) and bias-corrected online following the algorithm of Derber and Wu (1998). Furthermore, the GSI used in the experiments here includes the adjoint capability of Trémolet (2007, 2008).

This adjoint of GSI differs from its previous incarnation due to Zhu and Gelaro (2008) in that it is not a line-by-line adjoint, but rather it is derived from a swap of operations used in the forward GSI. Combining the GSI adjoint with the GCM adjoint, GEOS-5 has all the ingredients to calculate the approximations discussed earlier.

Two sets of experiments were performed and the results are discussed in what follows. In the first experimental setup, hereafter referred to as DAS-1, for compatibility with the assumptions in the theory presented in the previous sections, we replace the GEOS-5 two-outer loop GSI-based 3D-Var with a single outer loop. In this way nonlinearities in the observation operator and therefore in the  $\mathbf{K}$  operator are *avoided*. Accordingly, when the analysis adjoint is used, this first experiment, only executes a single outer loop of the adjoint analysis. The second experimental setup, hereafter referred to as DAS-2, leaves the default settings of the analysis minimization untouched, therefore using two outer loops to calculate analysis increments at each synoptic time. This experiment, essentially *ignores* the fact that  $\mathbf{K}$  is indeed nonlinear. In the DAS-1 setup first-order Taylor series and second-order quadrature measures in Table 1 are implemented for a single forecast in early February 2007; experiments in the DAS-2 setup compare  $\delta e$  to the trapezoidal and midpoint approximations and the observation impact estimations provided by these measures for a full month of forecasts, valid at 0000 UTC, in August 2007. All experiments are performed at a horizontal resolution of  $2.5^\circ \times 2^\circ$  with 72 hybrid levels in the vertical. The model functional aspect is specified as the 24-hours forecast error (4) with a diagonal matrix  $\mathbf{C}$  taken such that  $e$  measures the average global forecast error between the model vertical grid levels 40 to 72 (from the surface to approximately 128 hPa) in a total (dry) energy norm.

Over the time periods of interest, GEOS-5 DAS assimilates observations from the conven-

tional network: radiosondes; wind profilers; PIBAL winds; ASDAR and MDCARS aircraft wind and temperature reports; NEXRAD radar winds; dropsonde winds; PAOB surface pressure; GMS and METEOSAT cloud drift infrared (IR) and visible winds; MODIS clear sky and water vapor winds; GOES cloud drift IR and water vapor cloud top winds; surface land observations; SSM/I rain rates and wind speeds; TMI rain rates; and QuickSCAT wind speeds and directions. Satellite radiances include: TOVS level 1b AMSUA from NOAA-15, NOAA-16, and NOAA-18, AMSUB from NOAA-15, NOAA-16, and NOAA-17, HIRS-2 from NOAA-14, HIRS-3 from NOAA-16 and NOAA-17, MSU from NOAA-14; EOS/Aqua level 1b radiances AIRS and AMSUA; GOES-10 and GOES-12 sounders brightness temperatures; and SBUV-2 (version 6) layer and total column ozone from NOAA-16.

*a. Results in the DAS-1 setup*

In the DAS-1 setup the analysis state  $\mathbf{x}_a$  is obtained by assimilation of data valid at 0000 UTC 01 February 2007 and the verifying state  $\mathbf{x}^t$  is provided at 0000 UTC 02 February 2007 by performing 6-hour analysis cycles.

The parametric approach may be used to identify appropriate  $\delta e$ -approximation measures and to quantify the approximation error introduced by the evaluation of the derivatives in the observation space. Theoretically, given the relationships (18) and (20), approximations based on derivatives estimated in the parameter space are equivalent to approximations based on derivatives estimated in the observation space. As an alternative to (20), from (17) the derivatives  $\hat{e}'(s)$  may be estimated from nonlinear model forecasts and finite differences schemes. The graphs of the function  $\hat{e}(s)$  and of the derivative  $\hat{e}'(s)$  as the parameter  $s$  spans

the interval  $[0, 1]$  are displayed in Fig. 2. This information was obtained using nonlinear model forecasts initiated from  $\mathbf{x}(s) = \mathbf{x}_b + s\delta\mathbf{x}_a$  to evaluate  $\hat{e}(s) = e(\mathbf{x}(s))$  at an  $s$ -increment of 0.1 (a total of eleven forecasts were performed) and second order accurate finite differences schemes to estimate  $\hat{e}'(s)$ . At parameter value  $s = 0$ ,  $\hat{e}(0) = e(\mathbf{x}_b)$  and the average forecast error was found to be  $e(\mathbf{x}_b) = 9.80 \text{ J kg}^{-1}$ . At parameter value  $s = 1$ ,  $\hat{e}(1) = e(\mathbf{x}_a)$  and the average forecast error was found to be  $e(\mathbf{x}_a) = 6.75 \text{ J kg}^{-1}$ . The average forecast error reduction  $\delta e = -3.05 \text{ J kg}^{-1}$  is the overall impact of the observations in the data assimilation scheme, indicative of the effectiveness of assimilating observations as measured by the (dry) total energy norm. Insight on the  $\delta e$ -approximation measures is provided by the graph of the derivative  $\hat{e}'(s)$  in Fig. 2. The first order measure  $\delta e_1^b$  approximates  $\hat{e}'(s)$  in (26) by the constant value  $\hat{e}'(0)$ , whereas  $\delta e_1^a$  approximates  $\hat{e}'(s)$  by the constant value  $\hat{e}'(1)$ . The derivative  $\hat{e}'(s)$  exhibits a linear dependence on the parameter  $s$  and indicates that  $\hat{e}(s)$  is close to a quadratic function. Second-order measures are thus appropriate and are *expected* to provide accurate  $\delta e$ -approximations in these experiments.

It must be emphasized that the functionals  $\hat{e}(s)$  and  $\hat{e}'(s)$  provide only information regarding the approximation properties of the  $\delta e$ -measures and that observation impact studies require an observation-space evaluation of the derivatives. In practice, the accuracy in the adjoint-based  $\delta e$ -approximations is impaired by various simplifications used in the derivation and implementation of the adjoint model  $\mathbf{M}^T$  and/or the adjoint DAS operator  $\mathbf{K}^T$ . For example, the adjoint model is often run at a coarse resolution, as compared to the nonlinear forecast model, and may not properly account for moist physics or non-linearities in the dry dynamics (LB04). Issues in the development of an adjoint DAS that is fully consistent to the assimilation scheme are discussed in the work of Zhu and Gelaro (2008).

Table 2 provides the values of various  $\delta e$ -approximations based on finite differences derivative estimates in the parameter space and adjoint-based derivatives in the observation space. It is noticed that the second-order measures based on finite differences derivative estimation in the parameter space provided accurate approximations, whereas the observation-space computation of the derivatives introduced an approximation error of  $\sim 30\%$ . Relative errors of similar magnitude were reported in LB04 and GZE07. The adjoint relationship between the operators  $\mathbf{K}$  and  $\mathbf{K}^T$  was checked and proved to be valid and evaluating the  $\delta e$ -measures in the state space did not improved the estimates. Therefore, the increased uncertainty in the adjoint-based second-order  $\delta e$ -approximations is mainly due to inconsistencies between the nonlinear forecast model and the implementation of the adjoint model  $\mathbf{M}^T$ .

First- and second-order adjoint-based observation impact estimates and the corresponding estimates of the contribution of various observing system components to the average forecast error reduction are provided in Fig. 3. The observation impact is largely overestimated in the measure  $\delta e_1^b$  and largely underestimated in the measure  $\delta e_1^a$ . The second-order quadrature measures  $\delta e_2^{a,b}$  and  $\delta e_2^{(a+b)/2}$  provided consistent estimates of the impact of each observing system component. Based on the second-order estimates, the largest percentage contribution to the forecast error reduction is attributed to the radiance data (45%) and wind data (37%) followed by the temperature (12%) and surface pressure data (5%). The impact of other observations in the assimilation scheme such as humidity and ozone data was estimated to be less than 0.5%. Estimates based on the fourth-order measure  $\delta e_4^{a,b,(a+b)/2}$  (not shown) were in close agreement to the second-order estimates and it is noticed that  $\delta e_4^{a,b,(a+b)/2} = 1/3\delta e_2^{a,b} + 2/3\delta e_2^{(a+b)/2}$ . The use of the fourth order measure may be of interest in assessing the observation impact on forecasts beyond 24 hours when nonlinearities in the

model forecast may result in a large deviation from quadratic of the forecast error aspect.

*b. Results in the DAS-2 setup*

Our second illustration involves evaluating the trapezoidal and midpoint estimates for the calculation of observation impact on the 24-hour forecasts, valid at 0000 UTC, over the month of August 2007. Aside from resolution, this experiment mimics precisely the normal mode of execution of GEOS-5 DAS, where in particular, the analysis uses two outer loops for its minimization. Figure 4 shows the time series of the actual forecast error reduction  $\delta e$  (thin line) calculated directly from the differences between the 24-hour forecasts with the corresponding verifications (analyses), where the forecast errors are evaluated in terms of total (dry) energy. The actual forecast error reduction shown here is similar to that shown in Fig. 1 of GZE07, but now for a different time period. The 1-day forecast error reduction due to the assimilation of observations oscillates between  $1 \text{ J kg}^{-1}$  and  $3.5 \text{ J kg}^{-1}$ , with the negative sign indicating that the assimilation of observations improved the forecasts as a whole. Estimates from the second-order quadrature measures  $\delta e_2^{a,b}$  (trapezoidal) and  $\delta e_2^{(a+b)/2}$  (midpoint) are also displayed in Fig. 4, as indicated by the *X*- and *O*-marked lines, respectively. Both estimates are quite close to each other, and are reasonable approximations to the actual error reduction. At times, the trapezoidal calculation tends to get closer to the actual error reduction than the midpoint; at other times, this seems to reverse. Both estimates here are closer to the actual error reduction than what appears in GZE07. This is attributed mainly to the way the line-by-line adjoint of Zhu and Gelaro handles the analysis outer loop versus the adjoint of Trémolet (2007, 2008).

A more detailed examination is shown in Fig. 5 where the contribution of various observing systems to the forecast error reduction is displayed. The black bars are for the trapezoidal estimates; and the clear bars are for the midpoint estimates. Panel (a) shows the observation impacts in  $\text{J kg}^{-1}$ , and panel (b) shows the fractional observational impacts, i.e., the observation impacts divided by the total estimate and multiplied by 100. Both estimates are completely consistent. For example, they both show AMSUA being the dominant observing system when it comes to impacting the 24-hr forecasts, followed by the radiosonde and dropsonde observations. The trapezoidal estimate sees AMSUA contributing slightly less than the midpoint estimate; and reversely, the midpoint estimate sees the radiosonde and dropsonde network contributing slightly more to the reduction in forecast error than the trapezoidal estimate. These small differences between the two estimates become even less noticeable when considering the fractional impact (panel b). For all practical purposes, the existing subtle differences between the two estimates are negligible, particularly when viewed in the context of approximations such as the nonlinearity of  $\mathbf{K}$ , the lack of physics in the adjoint, to cite a few.

## 5. Conclusions and further work

This study provides insight on the adjoint-based observation impact measures implemented in NWP and contributes toward the development of a judicious theoretical framework to high-order observation impact estimates. In E07 it was first noticed that the  $\delta\mathbf{y}$ -amplification factor in the LB04 observation impact measure is not *per se* a gradient, but a weighted combination of two gradients and that a proper interpretation of this term needs

to be further investigated. The parametric approach allows an interpretation and analysis of the LB04 measure as a quadrature scheme to express the variation in the model functional output due to assimilation of data. Approximation formulae associated to standard numerical integration schemes were provided together with their order of accuracy and error estimates. The parametric approach provides a tool to assess the approximation properties of the  $\delta e$ -measures using nonlinear model forecasts. In practice, the accuracy of high-order adjoint-based measures is limited by the deficiencies in the current adjoint forecast models e.g., moist physical processes are not properly incorporated in the adjoint model.

An attractive feature of the quadrature methods is that high-order  $\delta e$ -approximations may be derived using gradients evaluated along trajectories properly initiated on the segment from  $\mathbf{x}_b$  to  $\mathbf{x}_a$ . Their potential drawback is that information from both ends of the integration interval is involved in the approximation formulae. Whether or not ambiguities are introduced when these schemes are used to estimate the impact of individual observations in the DAS needs to be further investigated and a judicious validation using OSE's needs to be performed.

The theoretical framework developed in this work is specialized to a linear analysis scheme and further research is needed in the design and implementation of high-order observation impact measures in nonlinear data assimilation. Computation of observation sensitivity and observation impact estimation in variational data assimilation (VDA) schemes with multiple outer loops is presented in the work of Trémolet (2008). The sensitivity equations of a 4D-Var DAS are discussed by Daescu (2008). An extension of the parametric approach to derive high-order  $\delta e$ -approximation measures for observation impact estimates in a nonlinear VDA scheme may be formulated using continuation theory for solving nonlinear equations and

optimization problems (Ortega and Rheinboldt 1970, Watson 2000, Dunlavy and O’Leary 2005) and it will be provided in a subsequent study.

*Acknowledgments.*

The numerical results in this work were obtained on the Linux Explore System through a cooperation with the NASA Center for Computational Sciences at Goddard Space Flight Center. The work of D.N. Daescu was supported by the NASA Modeling, Analysis, and Prediction Program under award NNG06GC67G. The work of R. Todling was partially supported by the Atmospheric Data Assimilation Development component of the NASA Modeling, Analysis, and Prediction Program (MAP/04-0000-0080). We thank two anonymous reviewers whose thoughtful comments and suggestions helped to improve the manuscript.

# APPENDIX

## On the observation impact measure $(1/2)\delta e_1^b$

In the study of GZE07 using the forecast error measure (4) it was found that  $\delta e_1^b$  largely overestimated the actual variation  $\delta e$ ,  $\delta e_1^a$  largely underestimated  $\delta e$ , and that a significantly improved approximation was obtained by taking  $(1/2)\delta e_1^b$ . While this estimate appears to have been first considered on an empirical basis, further insight is provided by Trémolet (2007) where it is shown that if the response functional  $e$  is quadratic as a function of the initial conditions (thus linear forecast model) and  $\mathbf{x}_a$  minimizes  $e$  (i.e.,  $\mathbf{x}_a^f = \mathbf{x}^t$ ) then  $\delta e = (1/2)\delta e_1^b$ .

From eqs. (9) and (14) one notices that, including the case of nonlinear dynamics,

$$\text{if } \nabla_{\mathbf{x}_0} e(\mathbf{x}_a) = 0 \text{ then } (1/2)\delta e_1^b = \delta e_2^{a,b} \tag{A1}$$

thus

*If the analysis  $\mathbf{x}_a$  is the initial state that (nearly) minimizes the model functional aspect i.e.,*

$$\mathbf{x}_a \simeq \text{Arg min}_{\mathbf{x}_0} e(\mathbf{x}_0) \tag{A2}$$

*then  $(1/2)\delta e_1^b$  is (nearly) equal to  $\delta e_2^{a,b}$  and the estimate  $\delta e \approx (1/2)\delta e_1^b$  is (nearly) second order accurate.* This situation may be encountered in idealized observation impact experiments when the functional aspect is defined as the variance of the error in the initial conditions and the specification of the matrices  $\mathbf{R}$  and  $\mathbf{B}$  is statistically consistent to the observation and

background errors, respectively. Most general, (A1) holds for *any* response functional  $e$  and merely requires  $\mathbf{x}_a$  to be a *stationary point* (initial condition) to the functional  $e$ ; for linear dynamics and quadratic  $e$ , in addition  $\delta e_2^{a,b} = (1/2)\delta e_1^b = \delta e$ . Loss of information will result when first order observation impact estimates are based on derivatives at (nearly) stationary points. It is also noticed that

$$\text{if } \nabla_{\mathbf{x}_0} e(\mathbf{x}_b) = 0 \quad \text{then} \quad (1/2)\delta e_1^a = \delta e_2^{a,b} \quad (\text{A3})$$

which applies to the quadratic functional

$$e(\mathbf{x}_0) = \frac{1}{2}(\mathbf{x}_0 - \mathbf{x}_b)^T \mathbf{C}(\mathbf{x}_0 - \mathbf{x}_b) \quad (\text{A4})$$

used in the study of Zhu and Gelaro (2008) and to the functional

$$e(\mathbf{x}_0) = (\mathbf{x}_0^f - \mathbf{x}_b^f)^T \mathbf{C}(\mathbf{x}_0^f - \mathbf{x}_b^f) \quad (\text{A5})$$

used in the study of Fourrié et al. (2002).

## REFERENCES

- Atkinson, K.E., 1988: *An Introduction to Numerical Analysis*. John Wiley & Sons, Inc., 693pp.
- Atlas, R., 1997: Atmospheric observations and experiments to assess their usefulness in data assimilation. *J. Meteorol. Soc. Japan*, **75**, No. 1B, 111–130.
- Baker, N.L., and R. Daley, 2000: Observation and background adjoint sensitivity in the adaptive observation-targeting problem. *Q.J.R. Meteorol. Soc.*, **126**, 1431–1454.
- Bloom, S.C., Takacs, L.L., da Silva, A. M., and D. Ledvina, 1996: Data assimilation using incremental analysis updates. *Mon. Wea. Rev.*, **124**, 1256–1271.
- Chou, M.-D., and M. J. Suarez, 1999: A shortwave radiation parameterization for atmospheric studies. *NASA Tech. Memo.*, 104606, Vol. 15, 40pp.
- Collins, N., Theurich, G., Deluca, C., Suarez, M., Trayanov, A., Balaji, V., Li, P., Yang, W., Hill, C., and A. da Silva, 2005: Design and implementation of components in the earth system modeling framework. *Intl. J. High Perform. Comput. Appl.*, **19**, 341–350.
- Courtier, P., Thepaud, J.N., and A. Hollingsworth, 1994: A strategy of operational implementation of 4D-Var using an incremental approach. *Q.J.R. Meteorol. Soc.* **120**, 1367–1388.

- Daescu, D.N., 2008: On the sensitivity equations of four-dimensional variational (4D-Var) data assimilation. *Mon. Wea. Rev.*, **136**, 3050–3065.
- Daley, R., 1991: *Atmospheric Data Analysis*. Cambridge University Press, 457pp.
- Derber, J.C., and A. Rosati, 1989: A global oceanic data assimilation technique. *J. Phys. Oceanogr.*, **19**, 1333–1347.
- Derber, J.C., and W.-S. Wu, 1998: The use of TOVS cloud-cleared radiances in the NCEP SSI analysis system. *Mon. Wea. Rev.*, **126**, 2287–2299.
- Doerenbecher, A., and T. Bergot, 2001: Sensitivity to observations applied to FASTEX cases. *Non. Proc. Geophys.*, **8**, 467–481.
- Dunlavy, D.M., and D.P. O’Leary, 2005: Homotopy optimization methods for global optimization. Sandia National Laboratories, Report SAND2005-7495, 32pp.
- Errico, R.M., 2007: Interpretations of an adjoint-derived observational impact measure. *Tellus*, **59A**, 273–276.
- Errico, R.M., Gelaro, R., Novakovskaia, E., and R. Todling, 2007: General characteristics of stratospheric singular vectors. *Meteorologische Zeitschrift*, **16**, No. 6, 621–634.
- Fourrié, N., Doerenbecher, A., Bergot, T., and A. Joly, 2002: Adjoint sensitivity of the forecast to TOVS observations. *Q.J.R. Meteorol. Soc.*, **128**, 2759–2777.
- Gelaro, R., Zhu, Y., and R.M. Errico, 2007: Examination of various-order adjoint-based approximations of observation impact. *Meteorologische Zeitschrift*, **16**, No. 6, 685–692.

- Giering, R., Kaminski, T., Todling, R., and S.-J. Lin, 2003: Generating the tangent linear and adjoint models of the DAO finite volume GCM's dynamical core by means of TAF. *Geophysical Research Abstracts*, **5**, 11680.
- Kalnay, E., 2002: *Atmospheric Modeling, Data Assimilation and Predictability*. Cambridge University Press, 364pp.
- Kelly, G., Thépaut, J.N., Buizza, R., and C. Cardinali, 2007: The value of observations. I: Data denial experiments for the Atlantic and the Pacific. *Q.J.R. Meteorol. Soc.*, **133**, 1803–1815.
- Kleespies, T.J., van Delst, P., McMillin, L.M., and J. Derber, 2004: Atmospheric transmittance of an absorbing gas. 6. OPTRAN status report and introduction to the NESDIS/NCEP Community Radiative Transfer Model. *Appl. Opt.*, **43**, 3103–3109.
- Koster, R.D., Suarez, M.J., Ducharne, A., Stieglitz, M., and P. Kumar, 2000: A catchment-based approach to modeling land surface processes in a GCM. Part I: Model structure. *J. Geophys. Res.*, **105** 24809–24822.
- Langland, R.H., 2005: Observation impact during the North Atlantic TReC-2003. *Mon. Wea. Rev.*, **133**, 2297–2309.
- Langland, R.H., and N.L. Baker, 2004: Estimation of observation impact using the NRL atmospheric variational data assimilation adjoint system. *Tellus*, **56A**, 189–201.
- Le Dimet, F.X., Navon, I.M., and D.N. Daescu, 2002: Second order information in data assimilation. *Mon. Wea. Rev.*, **130** (3), 629–648.

- Liu, J., and E. Kalnay, 2008: Estimation of observation impact without adjoint model in an ensemble Kalman filter. Paper 6.3A to *The 12th Conference on Integrated Observing and Assimilation Systems for Atmosphere, Oceans, and Land Surface (IOAS-AOLS)*. 88th American Meteorological Society Annual Meeting, New Orleans LA, January 20-24, 2008.
- Lin, S.-J., 2004: A vertically Lagrangian finite-volume dynamical core for global models. *Mon. Wea. Rev.*, **132**, 2293–2307.
- Moorthi, S., and M.J. Suarez, 1992: Relaxed Arakawa-Schubert: A parameterization of moist convection for general-circulation models. *Mon. Wea. Rev.*, **120**, 978–1002.
- Ortega, J.M., and W.C. Rheinboldt, 1970: *Iterative Solution of Nonlinear Equations in Several Variables*. Academic Press, Inc., 572pp.
- Rienecker, M.M., Suarez, M. J., Todling, R., Bacmeister, J., Takacs, L., Liu, H.-C., Gu, W., Sienkiewicz, M., Koster, R.D., Gelaro, R., and I. Stajner, 2008: The GEOS-5 Data Assimilation System - Documentation of Versions 5.0.1 and 5.1.0. *NASA TM 104606*, *Technical Report Series on Global Modeling and Data Assimilation*.
- Stieglitz, M., Ducharne, A., Koster, R.D., and M. J. Suarez, 2001: The impact of detailed snow physics on the simulation of snow cover and subsurface thermodynamics at continental scales. *J. Hydromet.*, **2**, 228–242.
- Trémolet, Y., 2007: First-order and higher-order approximations of observation impact. *Meteorologische Zeitschrift*, **16**, No. 6, 693–694.
- Trémolet, Y., 2008: Computation of observation sensitivity and observation impact in incremental variational data assimilation. *Tellus A*, DOI: 10.1111/j.1600-0870.2008.00349.x

Watson, L.T., 2000: Theory of globally convergent probability-one homotopies for nonlinear programming. *SIAM J. Optim.*, **11**, 761–780.

Wu, W.S., Purser, R.J., and D.F. Parrish, 2002: Three-dimensional variational analysis with spatially inhomogeneous covariances. *Mon. Wea. Rev.*, **130**, 2905–2916.

Zhu, Y., and R. Gelaro, 2008: Observation sensitivity calculations using the adjoint of the Gridpoint Statistical Interpolation (GSI) analysis system. *Mon. Wea. Rev.*, **136**, 335-351.

## List of Tables

- 1 Adjoint-based  $\delta e$ -approximations in a linear data assimilation scheme. A subscript is used to specify the order of accuracy of the approximation and a superscript is used to specify the trajectories involved in the computation. 32
- 2 Approximations to the average forecast error reduction  $\delta e$  ( $\text{J kg}^{-1}$ ) based on finite differences derivative estimates in the parameter space and adjoint-based derivative estimates in the observation space. 33

TABLE 1. Adjoint-based  $\delta e$ -approximations in a linear data assimilation scheme. A subscript is used to specify the order of accuracy of the approximation and a superscript is used to specify the trajectories involved in the computation.

Measure	Equation
Taylor series	
$\delta e_1^b$	$(\delta \mathbf{y})^T \mathbf{K}^T \nabla_{\mathbf{x}_0} e(\mathbf{x}_b)$
$\delta e_1^a$	$(\delta \mathbf{y})^T \mathbf{K}^T \nabla_{\mathbf{x}_0} e(\mathbf{x}_a)$
$\delta e_2^b$	$(\delta \mathbf{y})^T \mathbf{K}^T \nabla_{\mathbf{x}_0} e(\mathbf{x}_b) + (1/2)(\delta \mathbf{y})^T \mathbf{K}^T \nabla_{\mathbf{x}_0}^2 e(\mathbf{x}_b) \mathbf{K} \delta \mathbf{y}$
$\delta e_2^a$	$(\delta \mathbf{y})^T \mathbf{K}^T \nabla_{\mathbf{x}_0} e(\mathbf{x}_a) - (1/2)(\delta \mathbf{y})^T \mathbf{K}^T \nabla_{\mathbf{x}_0}^2 e(\mathbf{x}_a) \mathbf{K} \delta \mathbf{y}$
Numerical quadrature	
$\delta e_2^{a,b}$	$(\delta \mathbf{y})^T \mathbf{K}^T (1/2) [\nabla_{\mathbf{x}_0} e(\mathbf{x}_b) + \nabla_{\mathbf{x}_0} e(\mathbf{x}_a)]$
$\delta e_2^{(a+b)/2}$	$(\delta \mathbf{y})^T \mathbf{K}^T \nabla_{\mathbf{x}_0} e(\mathbf{x}_{(a+b)/2})$
$\delta e_4^{a,b,(a+b)/2}$	$(\delta \mathbf{y})^T \mathbf{K}^T (1/6) [\nabla_{\mathbf{x}_0} e(\mathbf{x}_b) + 4\nabla_{\mathbf{x}_0} e(\mathbf{x}_{(a+b)/2}) + \nabla_{\mathbf{x}_0} e(\mathbf{x}_a)]$

TABLE 2. Approximations to the average forecast error reduction  $\delta e$  ( $\text{J kg}^{-1}$ ) based on finite differences derivative estimates in the parameter space and adjoint-based derivative estimates in the observation space.

$\delta e$	derivative estimation	$\delta e_1^b$	$\delta e_1^a$	$\delta e_2^{a,b}$	$\delta e_2^{(a+b)/2}$	$\delta e_4^{a,b,(a+b)/2}$
-3.05	finite difference	-4.66	-1.32	-2.99	-3.06	-3.04
	adjoint-based	-5.88	-2.06	-3.97	-4.04	-4.02

## List of Figures

- 1 Illustration of the parametric approach to the estimation of the variation in the model functional output due to assimilation of data. 36
- 2 Evolution of the average forecast error function  $\hat{e}(s)$  (left) and its derivative  $\hat{e}'(s)$  (right) as the parameter  $s$  spans the interval  $[0, 1]$ . 37
- 3 First- and second-order adjoint-based estimations of the observation impact on the average forecast error reduction. The estimated impact of all observations (*all*) and of observing system components including radiances (*rad*), winds (*uw*), temperatures (*temp*), and surface pressures (*spr*). Units of  $\text{J kg}^{-1}$ . 38
- 4 Time series of forecast error reduction in GEOS-5 due to assimilation of observations for 0000 UTC 24-hour forecasts in August 2007. The thin line is for the actual error reduction, the *X*-marked line is for the estimate error reduction calculated using the trapezoidal formula, and the *O*-marked line is for when the midpoint formula is used instead. Units are  $\text{J kg}^{-1}$ . 39

5 Estimate observation impact (a), in  $\text{J kg}^{-1}$ , and fractional observation impact (b), in %, for various instruments for all 0000 UTC 24-hr forecasts in August 2007. The black bars are for trapezoidal estimates; the clear bars are for mid-point estimates. The abbreviations along the vertical axis stand for observations of: *Ships*, ships and buoy temperature, winds specific humidity, and near-surface pressure; *SatWind*, cloud-drift winds; *SSMIs*, Special Sensor Microwave/Imager wind speeds; *SBUV2*, Backscatter Ultraviolet Instrument total column ozone ; *RaobDsnd*, radiosonde and dropsonde temperature, winds, specific humidity; *Qscat*, Scatterometer winds; *MODIS*, Moderate-resolution Imaging Spectroradiometer clear sky and water vapor winds; *LandSfc*, land observations of temperature, winds, surface pressure, and specific humidity; *HIRS*, radiances from the High resolution Infrared Radiation Sounder (3) from NOAA-16 and 17; *GOESND*, radiances from the Geostationary Operational Environmental Satellites; *Aircraft*, aircraft temperature and winds; *AMSUA*, radiances from the Advanced Microwave Sounding Unit on the NOAA-15, 16 and 18; *AMSUB*, Advanced Microwave Sounding Unit from NOAA-15, 16 and 17, as well as on Aqua; *AIRS*, NASA Aqua, Atmospheric Infrared Sounders radiances.

40

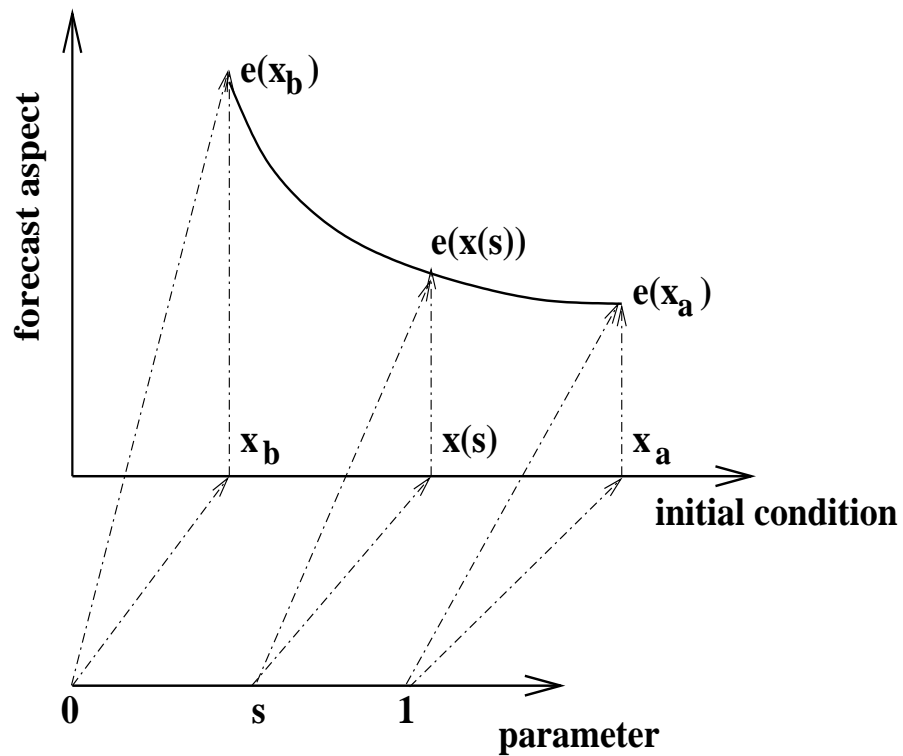


FIG. 1. Illustration of the parametric approach to the estimation of the variation in the model functional output due to assimilation of data.

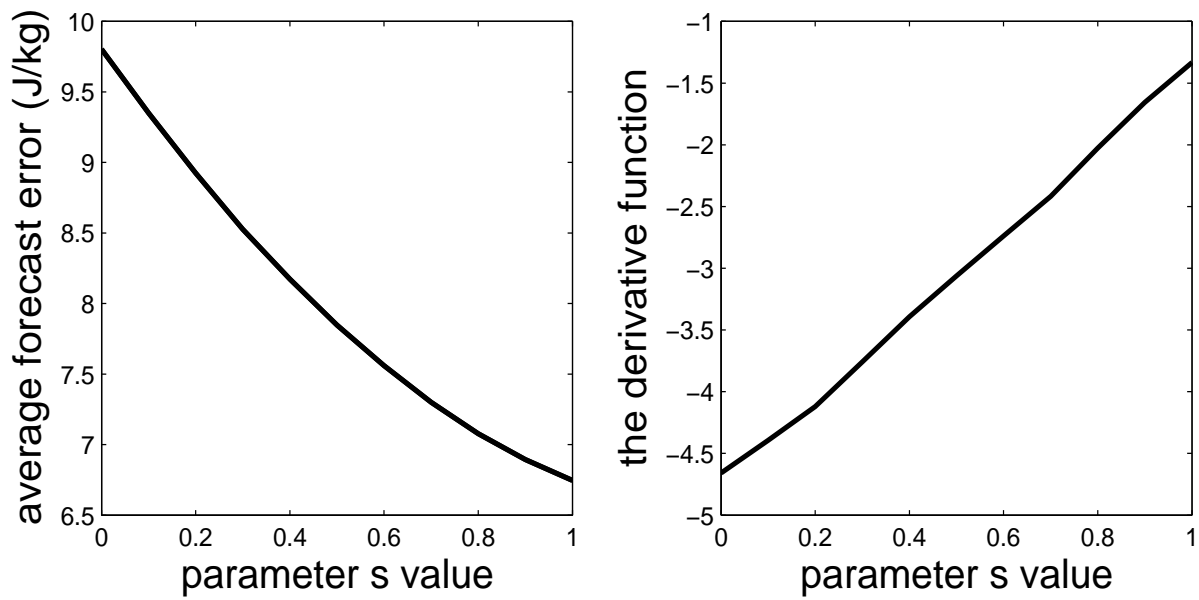


FIG. 2. Evolution of the average forecast error function  $\hat{e}(s)$  (left) and its derivative  $\hat{e}'(s)$  (right) as the parameter  $s$  spans the interval  $[0\ 1]$ .

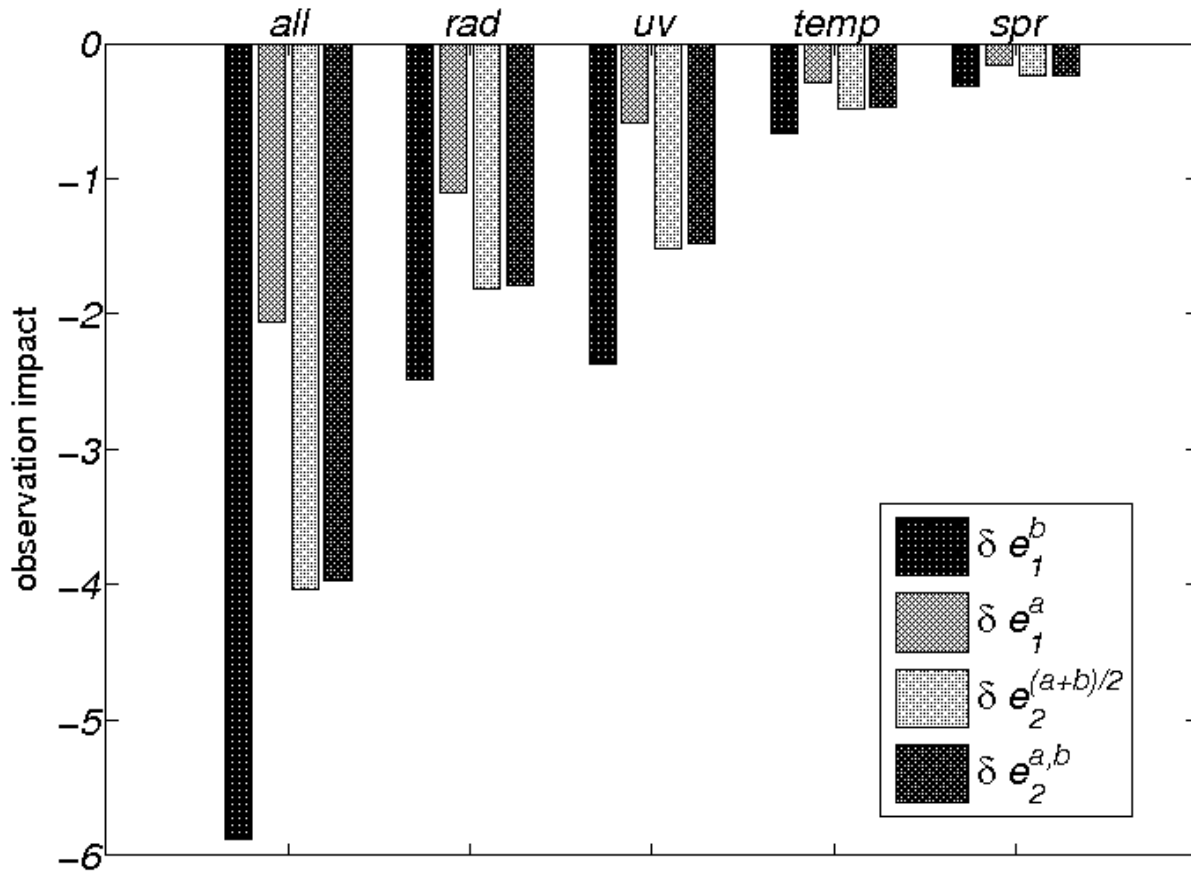


FIG. 3. First- and second-order adjoint-based estimations of the observation impact on the average forecast error reduction. The estimated impact of all observations (*all*) and of observing system components including radiances (*rad*), winds (*uv*), temperatures (*temp*), and surface pressures (*spr*). Units of  $\text{J kg}^{-1}$ .

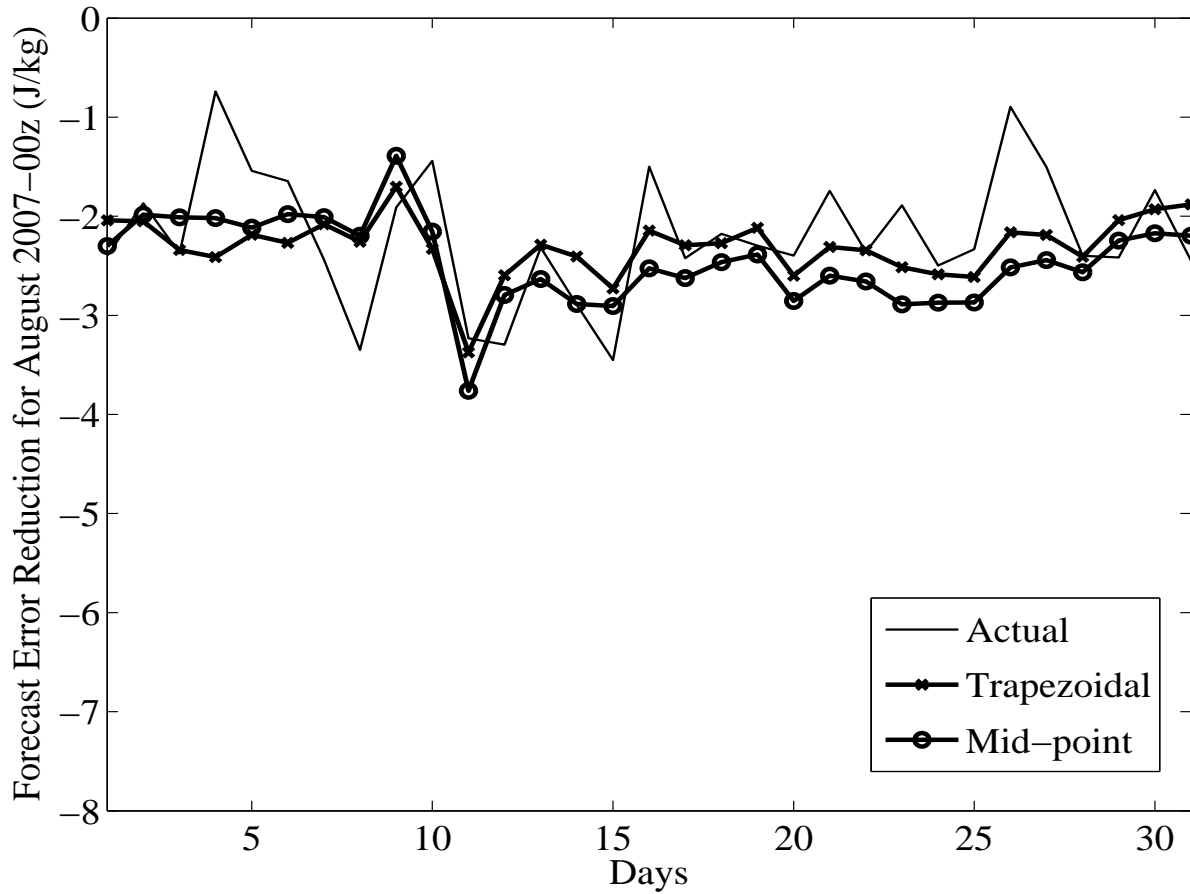


FIG. 4. Time series of forecast error reduction in GEOS-5 due to assimilation of observations for 0000 UTC 24-hour forecasts in August 2007. The thin line is for the actual error reduction, the  $X$ -marked line is for the estimate error reduction calculated using the trapezoidal formula, and the  $O$ -marked line is for when the midpoint formula is used instead. Units are  $\text{J kg}^{-1}$ .

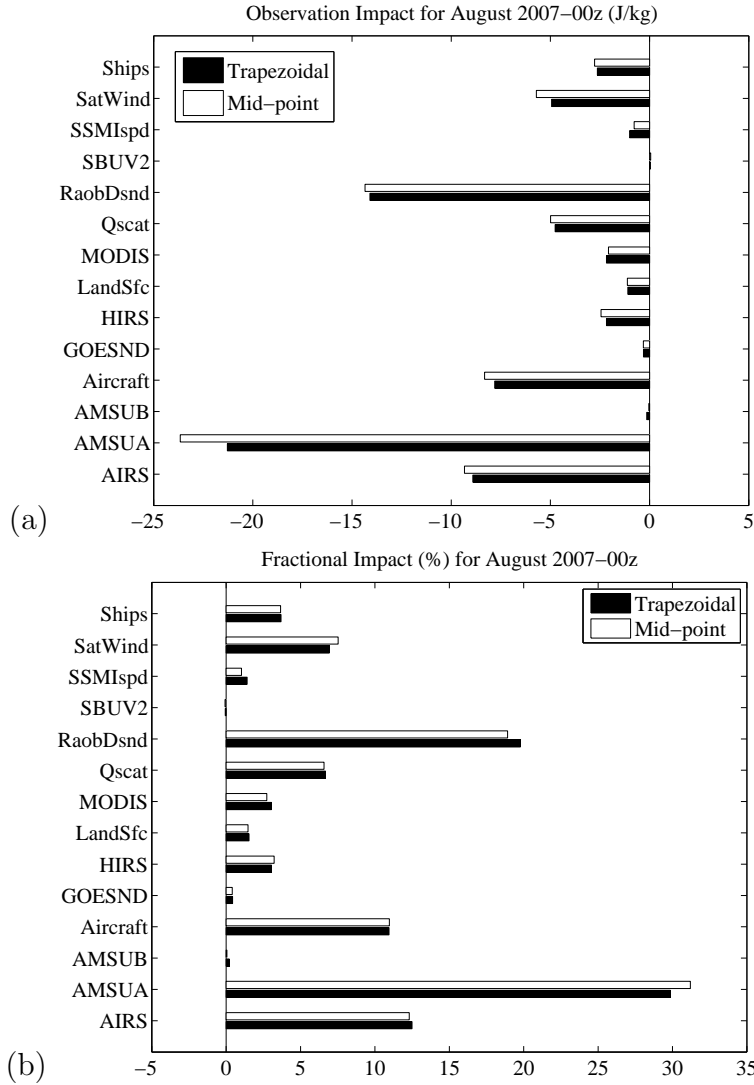


FIG. 5. Estimate observation impact (a), in  $J kg^{-1}$ , and fractional observation impact (b), in %, for various instruments for all 0000 UTC 24-hr forecasts in August 2007. The black bars are for trapezoidal estimates; the clear bars are for midpoint estimates. The abbreviations along the vertical axis stand for observations of: *Ships*, ships and buoy temperature, winds specific humidity, and near-surface pressure; *SatWind*, cloud-drift winds; *SSMIsPd*, Special Sensor Microwave/Imager wind speeds; *SBUV2*, Backscatter Ultraviolet Instrument total column ozone; *RaobDsnd*, radiosonde and dropsonde temperature, winds, specific humidity; *Qscat*, Scatterometer winds; *MODIS*, Moderate-resolution Imaging Spectroradiometer clear sky and water vapor winds; *LandSfc*, land observations of temperature, winds, surface pressure, and specific humidity; *HIRS*, radiances from the High resolution Infrared Radiation Sounder (3) from NOAA-16 and 17; *GOESND*, radiances from the Geostationary Operational Environmental Satellites; *Aircraft*, aircraft temperature and winds; *AMSUA*, radiances from the Advanced Microwave Sounding Unit on the NOAA-15, 16 and 18; *AMSUB*, Advanced Microwave Sounding Unit from NOAA-15, 16 and 17, as well as on Aqua; *AIRS*, NASA Aqua, Atmospheric Infrared Sounders radiances.